Struct Chem (2016) 27:1685–1692
DOI 10.1007/s11224-016-0804-z

ORIGINAL RESEARCH

Bergman, Bergman-based and 63-atom nanoclusters in intermetallics

T. G. Akhmetshina[1] · **V. A. Blatov**[1]

Received: 21 May 2016 / Accepted: 12 July 2016 / Published online: 26 July 2016

Abstract In this work, we apply the nanocluster method to analyze all known intermetallics containing two-shell nanoclusters with icosahedral core. Using the ToposPro program package, we have found all intermetallics with two-shell nanoclusters as building units or local configurations. We have analyzed in more details Bergman, Bergman-based and two types of icosahedral-based 63-atom nanoclusters, which have been discovered for the first time using the ToposPro nanoclustering procedure. Simplification of the nanocluster representations to their underlying nets revealed widespread topologies such as body-centered cubic (**bcu-x**), face-centered cubic (**fcu**) and hexagonal primitive (**hex**). We have performed topological analysis of these intermetallics in terms of local and overall binding of clusters. The statistical data on the chemical composition of the nanoclusters are presented; the ways of local binding of nanoclusters and the topology of the corresponding underlying nets are determined and classified.

Keywords Intermetallics · Nanocluster model · Icosahedral clusters · Bergman clusters

Dedicated to academician Vladimir Ya. Shevchenko on the occasion of his 75th birthday.

Electronic supplementary material The online version of this article (doi:10.1007/s11224-016-0804-z) contains supplementary material, which is available to authorized users.

✉ V. A. Blatov
blatov@samsu.ru;
http://sctms.ru/about/list/blatov-vladislav-anatolevich/

[1] Samara Center for Theoretical Materials Science (SCTMS), Samara National Research University, Ac. Pavlov St 1, Samara, Russia 443011

Introduction

The model of crystal structure as an assembly of nanosized building blocks has been known in materials science and crystallography for a long time. In the crystal chemistry of intermetallics, this model has been very productive [1, 2]. However, the building block approach faces at least two crucial problems: (1) many intermetallic compounds are too complicated to find their building blocks by visual analysis, and (2) usually the building blocks cannot be unambiguously chosen because of absence of strict criteria for their selection. To cope with these problems, we developed the strict 'Nanoclustering' procedure [3] and implemented it in the program package ToposPro [4]. Using this method, we have explored quite complicated intermetallic structures [3, 5]. In our recent work [6], we have applied a strict 'Nanoclustering' procedure [7] to create a database of the nanoclusters (fundamental configurations) that serve as building units in intermetallic structures. We used the database to classify the methods of assembly of intermetallics with simple (single-shell) icosahedron-based units.

It is known that icosahedral clusters are widespread in crystal structures of intermetallics. However, two-shell and multishell icosahedron-based structural units have not been analyzed in detail. The most common of them are Bergman and Mackay clusters, which were also discovered in quasicrystals and related structures [8]. In addition, a new type of two-shell 63-atom nanocluster with icosahedral core was recently described [9]. Up to now, it has been unknown how many intermetallics contain two-shell nanoclusters as building units. In this paper, we review intermetallic compounds consisting of Bergman, Bergman-based (containing Bergman cluster as a core) and 63-atom nanoclusters.

Experimental

For geometrical and topological analysis of intermetallics, we have used crystallographic data from the Inorganic Crystal Structure Database (ICSD, release 2015/2) [10] and Pearson's Crystal Data (version 2014/15) [11]. In total, these databases include more than 38,000 structures composed only by metal atoms. To find all crystal structures containing Bergman, Bergman-based and icosahedron-based 63-atom clusters (Fig. 1), we have used the collection of Topological Types of Nanoclusters (TTN) [6], which comprises information on 1006 polyhedral (single-shell) and 1011 multishell nanoclusters. In this way, we have found 285 intermetallics, in which the nanoclusters occur as local atomic configurations (structural fragments) irrespective of their role in the structure assembly. To find out whether the nanocluster is a structural unit that builds the intermetallic framework, we have used the 'Nanoclustering' procedure [7], which is based on the following rules:

1. The crystal structures of intermetallics are assembled of the *primary* nanoclusters, which can be polyhedral or multishell (onion-like). Interconnections between nanoclusters form the *supraclusters,* which characterize the local binding, and then the *underlying net*, i.e., the net of the centers of mass of the nanoclusters, which describes the global topology of the nanocluster assembly.
2. The set of primary nanoclusters should include all atoms of the crystal structure. However, in some cases, the structure may contain single atoms or small groups of atoms (*spacers*) that fill in voids between the primary nanoclusters. The number of such spacers should be minimal.
3. The centers of primary nanoclusters occupy the highest symmetry positions of the structure. It follows from the concept of fundamental configuration [3]; structural units should be as much regular as possible. The nanocluster can be non-centered (its center is empty), if it obeys principles (1)–(3).
4. The primary nanoclusters may have common external atoms, but they cannot interpenetrate. This rule restricts the size and the number of the primary nanoclusters. They are in fact considered as essentially independent regions in the structure organization, where any atom either belongs to only one region or is shared between boundaries of the regions.
5. If the structure has several different nanocluster models, all of them can be used to search for correlations with other structures. Nevertheless, according to the *parsimony principle,* the crystal structure should be assembled from minimal number of primary nanoclusters.

After applying the 'Nanoclustering' procedure, we have found that 23, 17 and one intermetallics can be represented as an assembly solely of Bergman, Berman-based and 63-atom clusters, respectively. In addition, 148 structures comprise these clusters along with other structural units. Out of the 148 structures, 137 and 11 contain Bergman and 63-atom primary nanoclusters, respectively. We denote the underlying nets with bold three-letter symbols of the Reticular Chemistry Structure Resource (RCSR) nomenclature [15]. To describe the method of local binding of nanoclusters, we have proposed [6] the descriptor $\text{Center@shell}^{\text{CN}}_{v,e,f,b}$, where center = 1 (centered nanocluster) or 0 (non-centered nanocluster), shell is the number of atoms in the nanocluster shell or the shell type, CN is the coordination number of the given nanocluster, and the subscript indices show the type of the nanocluster connection: by common vertices (*v*), edges (*e*), faces (*f*) or through metal–metal bonds (*b*) if the nanoclusters have no common atoms. In this paper, we use the symbols *ico*, *D*32 and *D*50 to designate icosahedral, 32-atom and 50-atom deltahedral shells, respectively.

For instance, the Cr_5Al_8 crystal structure [16] can be represented as an assembly of Bergman clusters. The

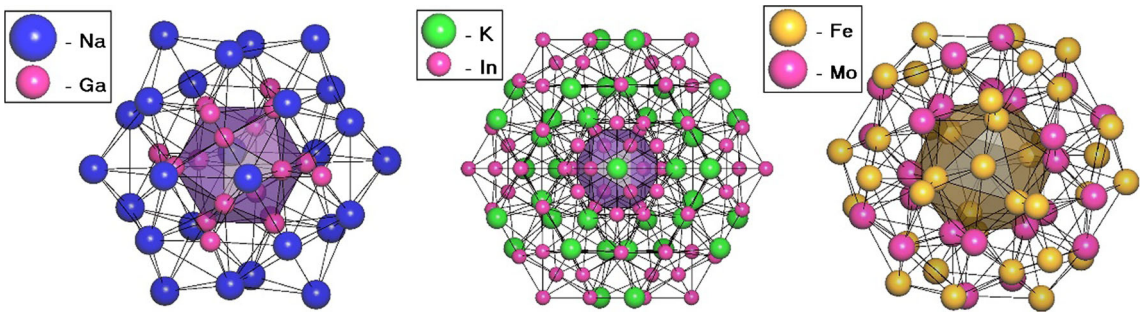

Fig. 1 Bergman (*left*), Bergman-based (*middle*) and icosahedron-based 63-atom (*right*) clusters in the Na_7Ga_{13} [12], $K_{39}In_{80}$ [13] and $Fe_{3.3}Mo_2$ [14] crystal structures, respectively; the information is stored in the TTN collection [6]. Additional projections of the nanoclusters are shown in Table S3

clusters are packed into an extended 14-coordinated body-centered cubic (**bcu-x**) underlying net. Each Bergman cluster is connected to six clusters by two triangular faces, to two clusters by six triangular faces and to remaining six by edges; the resulting symbol of local binding is $1@ico@D32^{6+2+6}_{f_3^2+f_3^6+e^1}$ (Fig. 2).

If the nanocluster model consists of two or more nanoclusters, the expanded descriptor should be used. Thus, the $Co_{0.442}Cr_{0.176}Mo_{0.382}$ crystal structure [17] is formed by two non-equivalent nanoclusters. The first one is a centered 63-atom icosahedron-based nanocluster, and the second one is a non-centered eight-vertex polyhedron. In this case, the local topology is described by two symbols: $1@ico@D50\left\{[0@8]^6_{v^1}+[1@ico@D50]^6_{f_3^2}\right\}$ and $0@8\left\{[1@ico@D50]^6_{v^1}\right\}$. It means that the 63-atom nanocluster is connected to six other nanoclusters through common triangular faces ($[1@ico@D50]^6_{f_3^2}$) and to six eight-vertex polyhedra by common vertices ($[0@8]^6_{v^1}$). Each eight-vertex polyhedron is connected only to 63-atom clusters via six vertices, respectively (Fig. 3).

Results and discussion

In this paper, we consider in detail the 41 intermetallics that are built just of one type of the two-shell nanoclusters. Complete statistical data on chemical composition, local

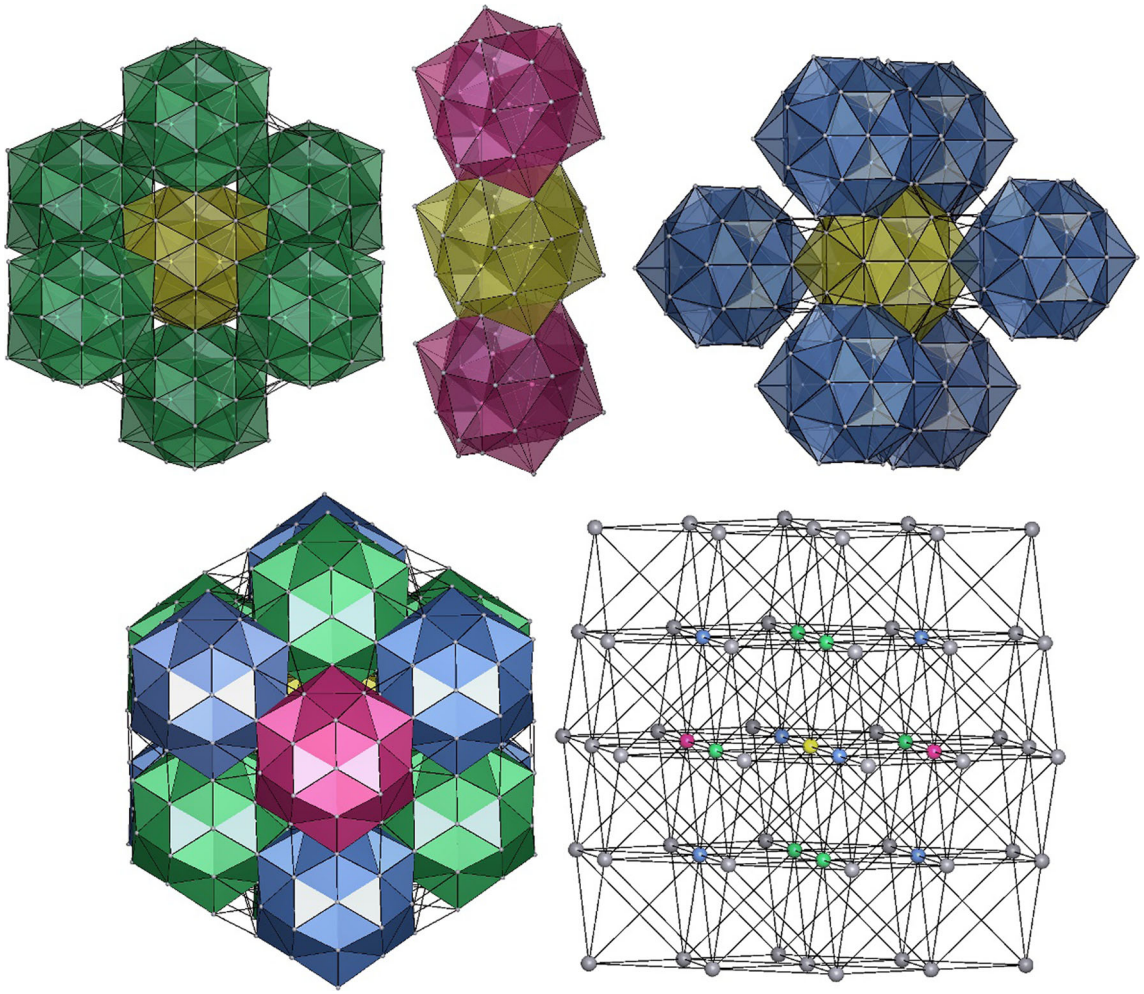

Fig. 2 (*Top*) Cr_5Al_8 crystal structure: connection of the Bergman clusters through two triangular faces (*left*), through six triangular faces (*middle*) and through one edge (*right*); (*bottom*) the result of the condensation of the Bergman clusters in a $1@ico@D32^{6+2+6}_{f_3^2+f_3^6+e^1}$ supracluster (*left*) and the corresponding **bcu-x** underlying net; the centers of the clusters that compose the supracluster are highlighted by the corresponding *colors* (*right*)

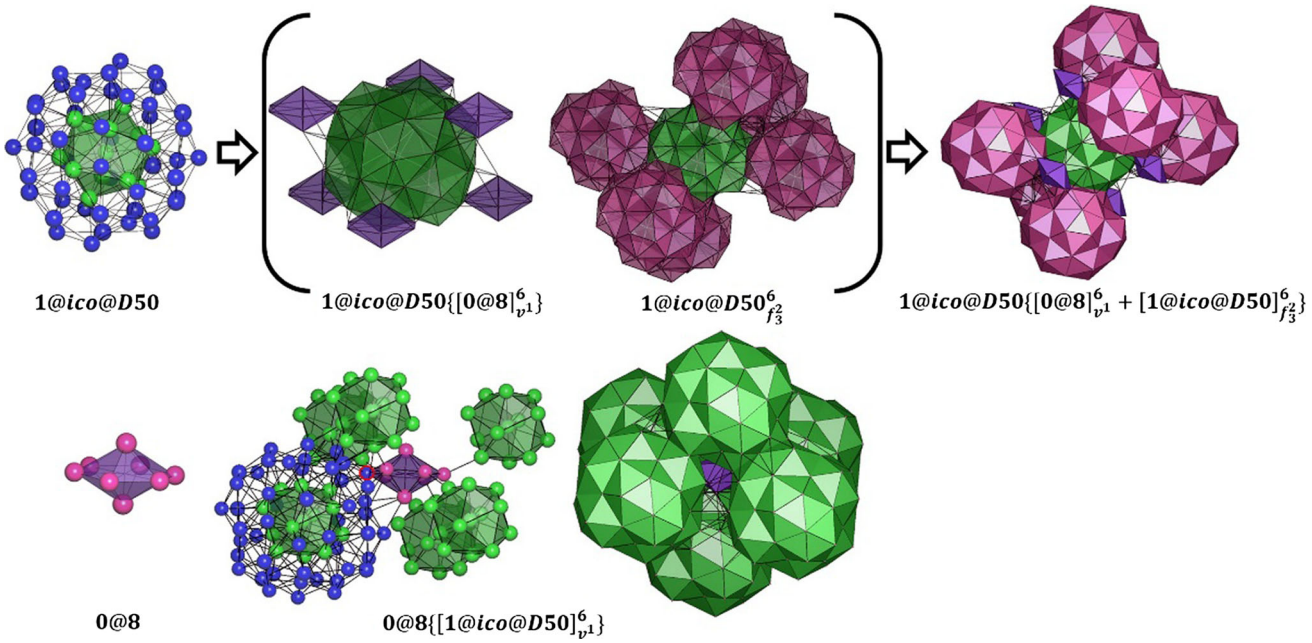

Fig. 3 (*Top*) Centered 63-atom icosahedron-based nanocluster (*left*) and the constituents (*middle*) of the corresponding supracluster (*right*); (*bottom*) non-centered eight-vertex polyhedron (*left*) is surrounded by six 63-atom clusters through vertices (*middle and right*)

binding and global topology of these intermetallics are given in Table S1 of the Supporting Information.

63-atom nanoclusters

With the TTN collection, we have found that four isomeric 63-atom nanoclusters occur in 60 topological types of intermetallic compounds, and only two models of these nanoclusters contain icosahedral inner polyhedron—1@12@50_model3 and 1@12@50_model4 with symmetry T_h and D_{3d}, respectively (Fig. 4). The $Ta_{1.108}Al$ structural type [20] can be represented as an assembly of the 63-atom nanoclusters (model_3), while the $Mo_{0.38}Cr_{0.16}Co_{0.46}$ crystal structure and seven other intermetallics belonging to the same topological type are assembled of two types of nanoclusters (Table S1). In the latest determination of the $Ta_{1.108}Al$ crystal structure [21], the authors mentioned the presence of the 63-atom cluster, but their description of the local and overall topologies differs from ours. The authors characterized the underlying net as the body-centered cubic motif, while we have determined that the nanoclusters are packed into a 12-coordinated underlying net according to the face-centered cubic (**fcu**) motif. The local binding is described by the symbol $1@ico@D50^{4+4+4}_{f_3^3+f_3^2+v^1}$, which means that the centered nanocluster with icosahedral (ico) first shell and deltahedral 50-atom second shell is connected to eight other nanoclusters through three or two common triangular faces and to four nanoclusters through one common vertex ($1@ico@D50^{4}_{v^1}$) (Fig. 5). The 63-atom nanocluster with configuration 1@12@50_model4 occurs in intermetallics as a building unit, but it always forms crystal structures with other two-shell nanoclusters. We have already considered the corresponding crystal structures in detail [10, 11].

Bergman-based intermetallics

In our previous work, we discussed Bergman and Bergman-based intermetallic compounds in brief [6, 22]. A surprisingly large amount of intermetallics can be described as an assembly of Bergman clusters: four topological types and 22 crystal structures. Empty three-shell Bergman-based nanoclusters form 17 crystal structures of the same topological type. Below, we consider the ways of the local and overall binding and chemical composition of the nanoclusters, which build these crystal structures.

Rb_3Hg_{20}, $Na_4K_6Tl_{13}$ type: 6 entries

In the Rb_3Hg_{20} structural type, the authors missed almost ideal Bergman cluster with the center in the 2*a* Wyckoff position [23]. The authors of the $Na_4A_6Tl_{13}$ structural investigation (A=K, Cs, Rb) [24] noted the icosahedral clusters and considered their second shells, but did not detected them as Bergman clusters. Our topological analysis revealed that the Bergman clusters are packed into a $1@ico@D32^{8+6}_{f_3^6+f_3^2}$ supracluster, and the resulting topology of the underlying net is 14-coordinated **bcu-x**. The method of the connection of the nanoclusters is shown in Fig. 6.

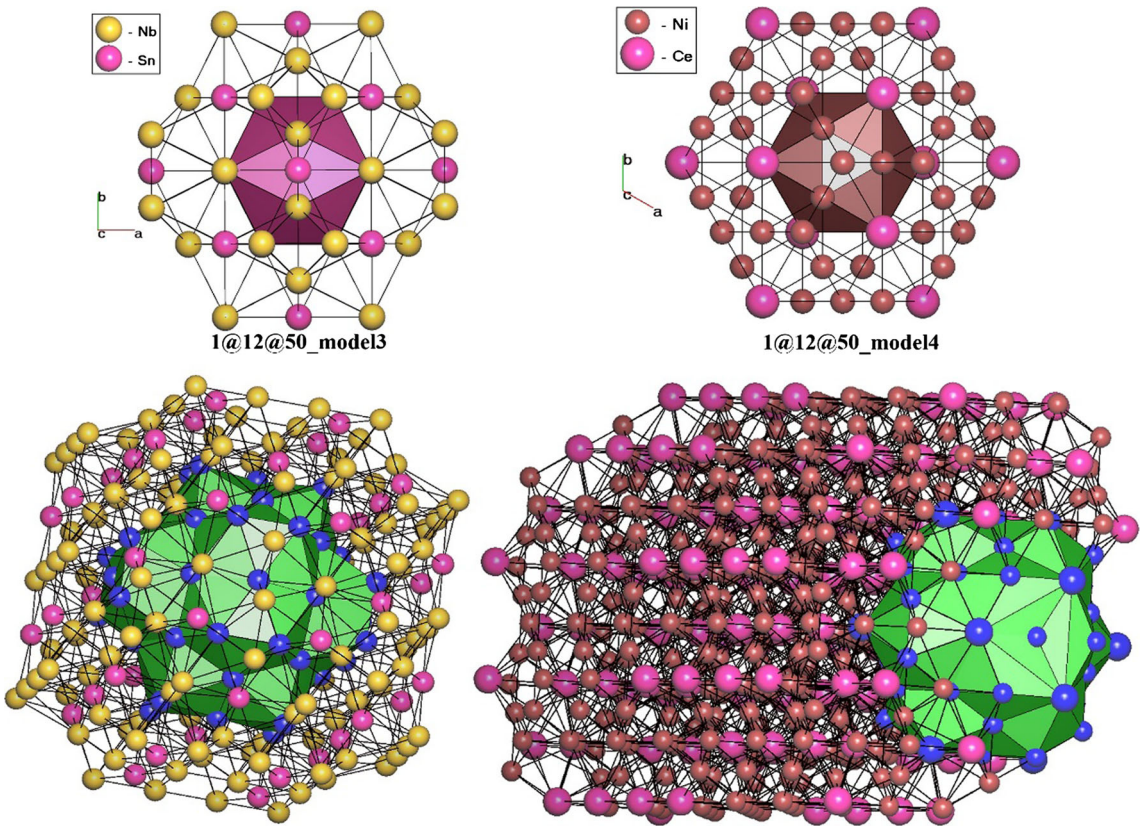

Fig. 4 (*Top*) Two types of 63-atom clusters with icosahedral core with T_h (*left*) and D_{3d} (*right*) symmetry which occur in the $(In_{0.25}Sn_{0.75})Nb_3$ [18] and Ce_2Ni_7 [19] crystal structures as local configurations; (*bottom*) clusters are selected in the corresponding crystal structures

Cr_5Al_8 type: 12 entries

Here, we can see an example of the so-called local topological isomerism: As in the previously described structures, the overall topology is **bcu-x**, but the local binding is not the same. In crystal structures of the Cr_5Al_8 type [16], each Bergman cluster is connected to six other clusters through two triangular faces ($1@ico@D32^6_{f_3^2}$), to two clusters through six faces ($1@ico@D32^2_{f_3^6}$) and to the remaining six clusters through edges ($1@ico@D32^6_{e^1}$) (Fig. 2).

$Na_3K_8Tl_{13}$ type: 1 entry

The $Na_3K_8Tl_{13}$ crystal structure [24] consists of the Bergman clusters, which form a supracluster with the local binding symbol $1@ico@D32^{6+6}_{f_3^5+f_3^2}$. The nanoclusters are assembled according to a 12-coordinated face-centered cubic (**fcu**) motif (Fig. 7).

$Sm_{12}Fe_{14}Al_5$ type: 1 entry

The unique structural type of $Sm_{12}Fe_{14}Al_5$ [25] can be represented as an assembly of Bergman clusters (center = Fe) with Al spacers filling the voids. Condensation of the Bergman clusters produces a supracluster $1@ico@D32^{6+2}_{f_3^2+f_3^5}$: The Bergman clusters are connected to each other via triangular faces as shown in Fig. 8. Such coordination of the clusters corresponds to the hexagonal primitive packing (**hex**). It should be noted that the authors of the original paper found icosahedra around Fe atoms, but missed the two-shell nanoclusters; this situation is quite widespread in the structural descriptions of the intermetallics under consideration.

$CaCd_6$ type: 17 entries

In [6], we have found the crystal structures belonging to the $CaCd_6$ type [26], which can be considered as completely assembled from three-shell Bergman-based nanoclusters 0@12@32@102. In all other eight topological types containing Bergman-based nanoclusters [6], the nanocluster models include other structural units. The Bergman-based nanocluster in $CaCd_6$ is surrounded by eight other nanoclusters through 14 triangular faces and by six nanoclusters through two triangular faces; the topology of the underlying net is **bcu-x**. It is noteworthy

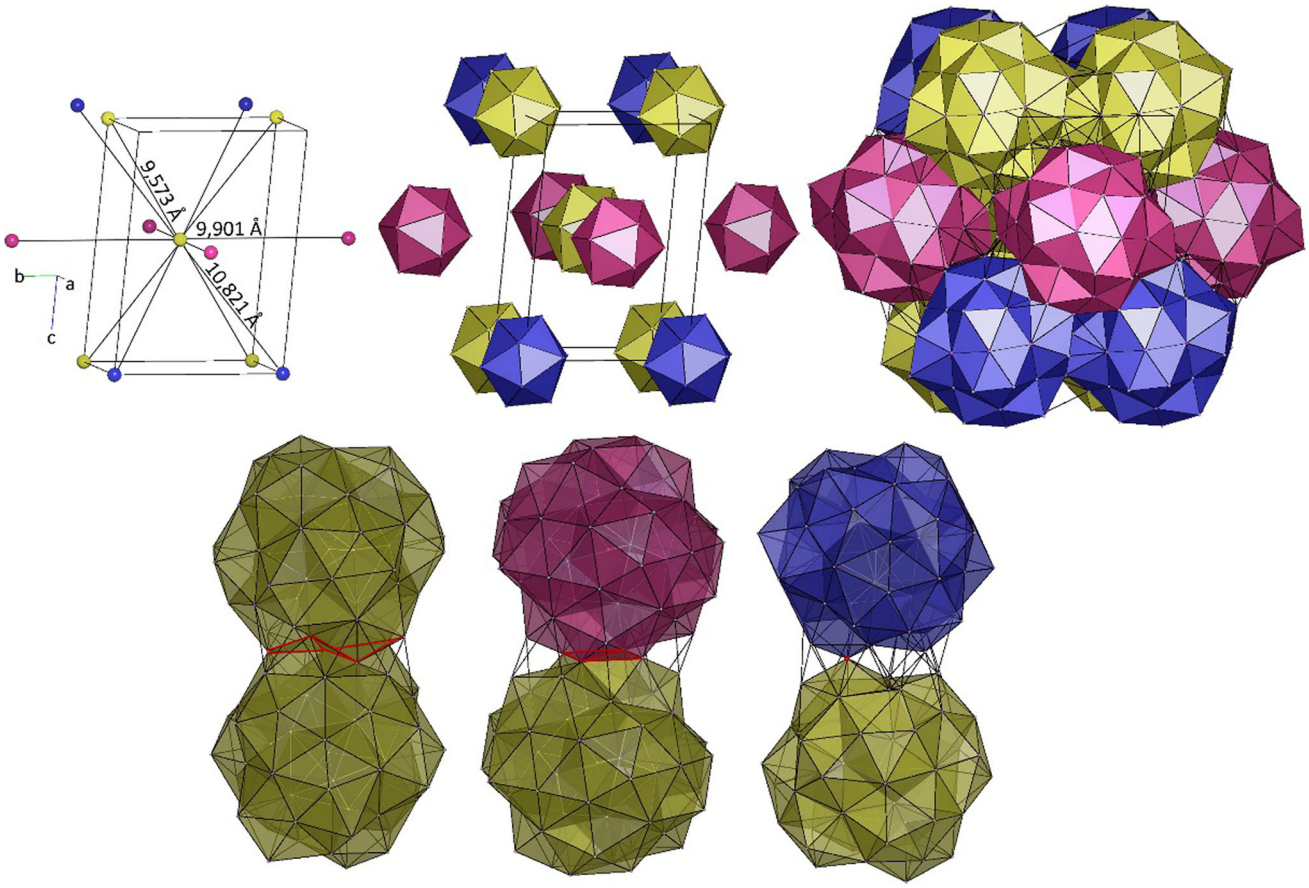

Fig. 5 Assembly of the $Ta_{1.108}Al$ crystal structure [20] with nanoclusters: (*top*) The Al22 atoms occupy the centers of the 63-atom nanoclusters (*left*) with icosahedral first shells (*middle*) that form the $1@ico@D50^{4+4+4}_{f_3^3+f_3^2+v^1}$ supracluster (*right*); each group of atoms that highlighted in *yellow*, *pink* and *blue* has equal distances to the central atom; (*bottom*) the central nanocluster is connected to the surrounding ones through three (*left*) and two triangular faces (*middle*) and one vertex (*right*), the common faces and vertex are highlighted in *red* (Color figure online)

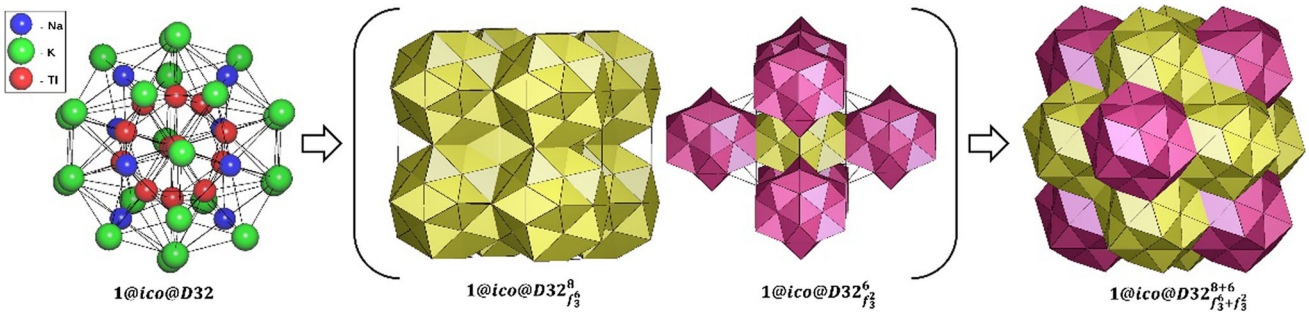

Fig. 6 Bergman cluster in the $Na_4K_6Tl_{13}$ crystal structure [24] with the centered inner icosahedron (*left*) and the constituents (*middle*) of the $1@ico@D32^{8+6}_{f_3^6+f_3^2}$ supracluster (*right*), where the central Bergman cluster is connected to the surrounding ones through six and two triangular faces

that the MCd_6 quasicrystal approximants have many different descriptions [27–29], but this three-shell Bergman-based building unit has not been detected so far.

Analysis of the chemical composition of the nanoclusters

We have analyzed the chemical composition of the nanoclusters, which assemble the crystal structures mentioned above;

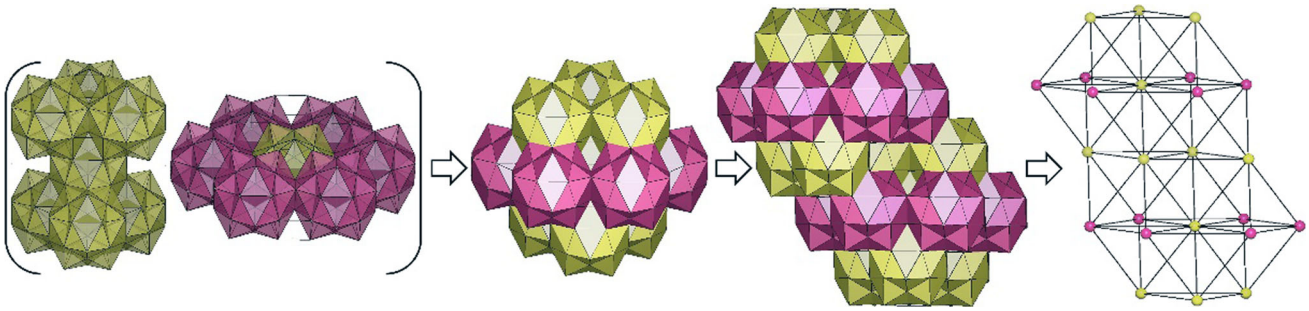

Fig. 7 $Na_3K_8Tl_{13}$ crystal structure [24]: the formation (*left*) of the $1@ico@D32^{6+6}_{f_3^5+f_3^2}$ supracluster (*middle*), where the central Bergman cluster is connected to the surrounding ones through faces, and the condensation of the supraclusters into a 12-coordinated **fcu** framework (*right*)

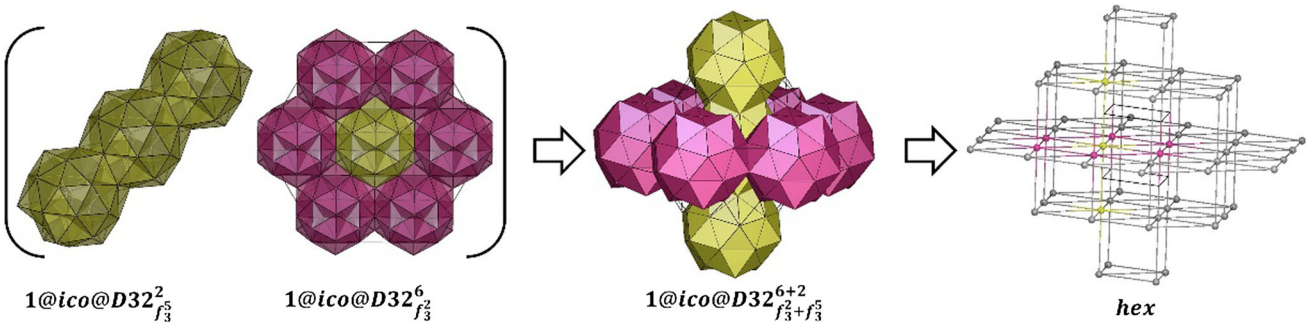

Fig. 8 Formation (*left*) of the $1@ico@D32^{6+2}_{f_3^2+f_3^5}$ supracluster (*middle*) in the $Sm_{12}Fe_{14}Al_5$ crystal structure [25]; the Bergman clusters are assembled according to a eight-coordinated hexagonal primitive lattice (**hex**) motif (*right*)

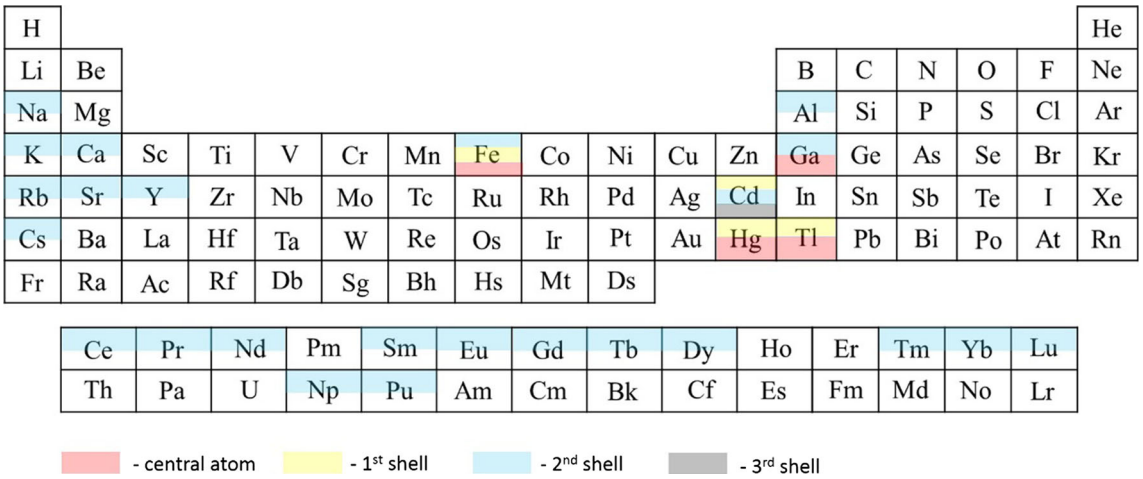

Fig. 9 Atoms that can form different shells of Bergman clusters: the central atoms, atoms of first, second and third shells are highlighted in *red*, *yellow*, *blue* and *gray colors*, respectively (Color figure online)

only completely ordered crystal structures were included in the statistical dataset. The first peculiarity is that the first shell of Bergman clusters consists of one sort of atoms in all cases. Even if we consider disordered structures, there are no exceptions: The first shell is always homogenous. The composition of the second shell is more ambiguous; there are five kinds of composition: $M1_8 + M2_{24}$, $M1_{12} + M2_{20}$, $M1_{30} + M2_2$ and $M1_{24} + M2_6 + M3_2$. As shown in Fig. 9, only Tl, Hg, Ga and Fe can be central atoms of Bergman clusters. The same elements and Cd can form the first shell. The second shell can consist of a wide range of elements: Al, Ga, Na, K, Rb, Cs, Cr, Fe, Cd, Ca, Sr, Y as well as some lanthanides and actinides. The third shell of Bergman-based nanocluster (in $CaCd_6$) is homogeneous and contains only Cd atoms.

Concluding remarks

In this paper, we have demonstrated the advantages of the nanocluster approach in modeling and analysis of complicated intermetallic structures. This approach allows one to automatically decompose the structure to multishell onion-like structural units (nanoclusters or fundamental configurations) and determine the method of their assembly. Using the nanocluster model, one can easily find structural correlations and regularities, which are usually missed in visual analysis. The results of the nanocluster analysis can be stored in electronic databases and used for the classification of other intermetallics. In particular, we are planning to use the ToposPro TTN collection and the data obtained here to systematic analysis of another important group of intermetallics built of two-shell Mackay nanoclusters.

Acknowledgments The authors are grateful to the Russian Government (Grant 14.B25.31.0005) for support.

References

1. Nyman H, Andersson S (1979) Acta Cryst A35:580–583
2. Lord EA, Mackay AL, Ranganathan S (2006) New geometries for new materials. Cambridge University Press, Cambridge
3. Shevchenko V. Ya., Blatov V. A., Ilyushin G. D. (2009) Struct Chem 20: 975 – 982
4. Blatov VA, Shevchenko AP, Proserpio DM (2014) Cryst Growth Des 14: 3576. http://topospro.com
5. Blatov VA, Ilyushin GD, Proserpio DM (2010) Inorg Chem 49:1811–1818
6. Pankova AA, Akhmetshina TG, Blatov VA, Proserpio DM (2015) Inorg Chem 54:6616–6630
7. Blatov VA (2012) Struct Chem 23:955–963
8. Steurer W, Deloudi S (2008) Acta Cryst A64:1–11
9. Shevchenko VY, Blatov VA, Ilyushin GD (2013) Glass Phys Chem 39:229–234
10. Belsky A, Hellenbrandt M, Karen VL, Luksch P (2002) Acta Cryst B58:364–369
11. Villars P, Cenzual K (2009) Pearson's crystal data crystal structure database for inorganic compounds (on CD-ROM). ASM International, Materials Park, OH
12. Frank-Cordier U, Cordier G, Schäfer H (1982) Z Naturforsch 37:119–127
13. Li B, Corbett JD (2003) Inorg Chem 42:8768–8772
14. Van der Kraan AM, Buschow KHJ (1986) Phys B 138:55–62
15. O'Keeffe M, Peskov MA, Ramsden SJ, Yaghi OM (2008) Acc Chem Res 41: 1782–1789. http://rcsr.anu.edu.au/
16. Brandon JK, Pearson WB, Riley PW, Chieh C, Stokhuyzen R (1977) Acta Cryst B33:1088
17. Komura Y, Sly WG, Shoemaker DP (1960) Acta Cryst 13:575
18. Otto G (1968) Z Phys 215:323–334
19. Cromer DT, Larson AC (1959) Acta Cryst 12:855–859
20. Boulineau A, Joubert JM, Černy R (2006) J Solid State Chem 179:3385–3393
21. Conrad M, Harbrecht B (2007) Philos Mag Lett 87:493–503
22. Blatov VA, Ilyushin GD, Proserpio DM (2011) Inorg Chem 50:5714–5724
23. Todorov E, Sevov SC (2000) J Solid State Chem 149:419–427
24. Zhen-Chao D, Corbett DJ (1995) J Am Chem Soc 117:6447–6455
25. Mizusaki S, Kawamura N, Taniguchi T, Nagata Y, Ozawa TC, Sato A, Noro Y, Samata HJ (2010) Magn Magn Mater 322:L19–L24
26. Johnson I, Schablaske R, Tani B, Anderson K (1964) Trans Met Soc AIME 230:1485–1486
27. Tsai AP, Guo JQ, Abe E, Takakura H, Sato TJ (2000) Nature 408:537–538
28. Gomez CP, Lidin S (2003) Phys Rev B 68:024203
29. Takakura H, Gomez CP, Yamamoto A, De Boisieu M, Tsai AP (2007) Nat Mater 6:58–63